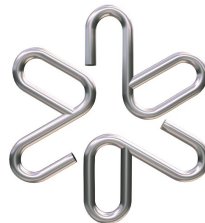# **Física do Corpo Humano**
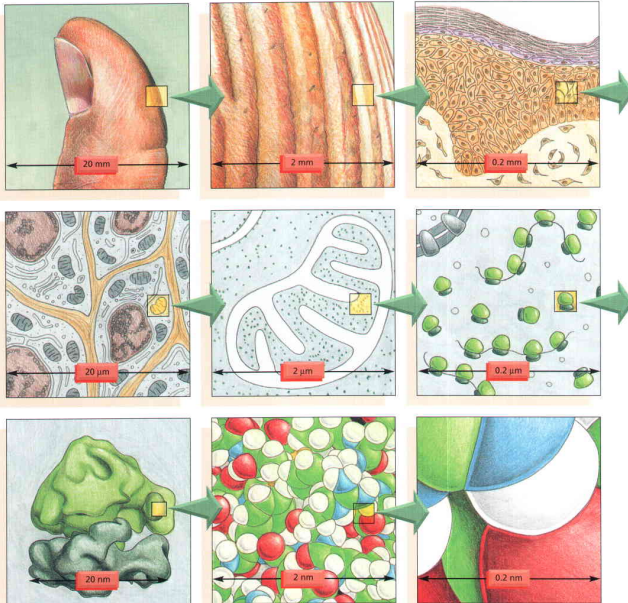## **(Física aplicado a Fisiologia)**

Adriano M. Alencar

Laboratório de Microrreologia e fisiologia Molecular (LabM²)
Departamento de Física Geral
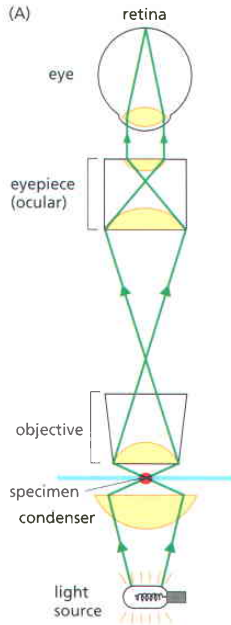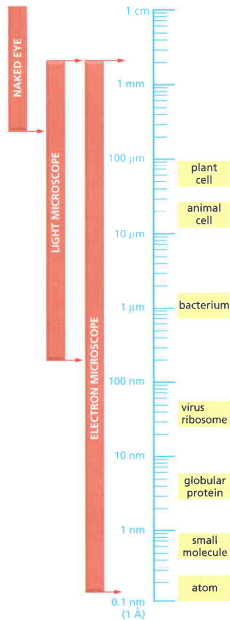Instituto de Física
Universidade de São Paulo
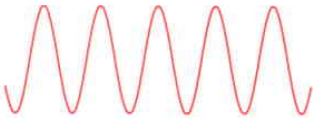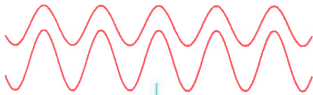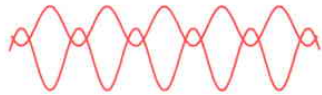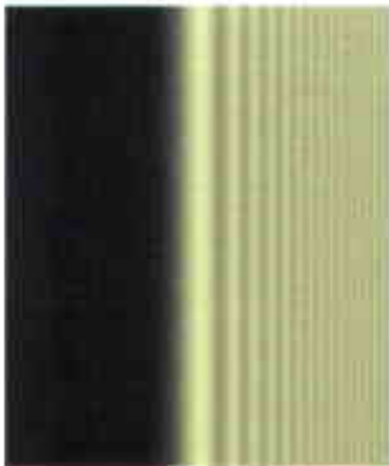
1 de abril de 2013

TWO WAVES IN PHASE

TWO WAVES OUT OF PHASE

BRIGHT

DIM

A resolução de um sistema pode ser limitado por dois fatores de origens diferentes e não correlacionados:

- aberração (morfológica ou cromática explicada via óptica geométrica). Pode ser solucionado \$\$\$
- difração (originado devido a natureza ondulatória da luz e determinado pela abertura finita dos elementos ópticos)

A resolução angular de um sistema óptico pode ser estimado pelo critério de Rayleigh [Lord Rayleigh: 12 de Novembro de 1842 - 30 de Junho de 1919]. Dois pontos são considerados minimamente resolvidos quando o máximo principal da difração de uma imagem coincide com o primeiro mínimo de uma outra imagem. Considerando a difração de uma onda λ, por uma abertura circular de diâmetro *D*:

$$\sin \theta = 1.220 \frac{\lambda}{D}$$

Onde θ é a resolução angular.
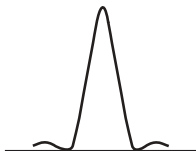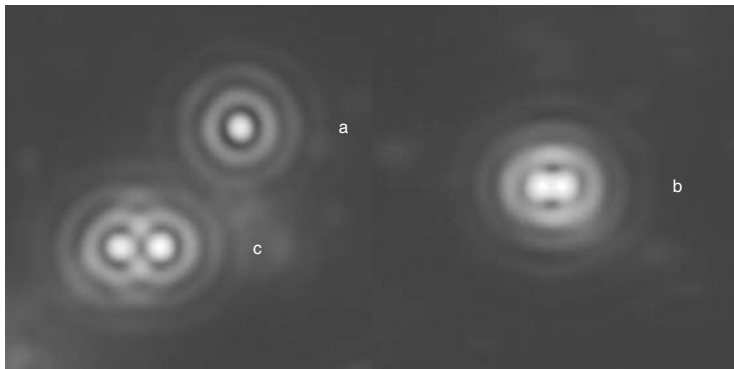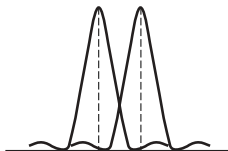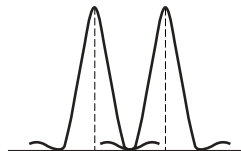
(a) (b) (c)

O fator 1.22 vem de um cálculo da posição do primeiro circulo escuro em torno de um disco de Airy (1.22 é aproximadamente o primeiro zero da Função de Bessel de primeiro tipo, de ordem 1, (J_1) dividido por π.
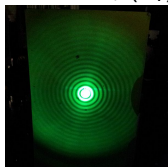
A resolução de um microscópio é medida em distância:

$$R = 1.220 \frac{\lambda}{NA_{\text{condensador}} + NA_{\text{objetiva}}}, \quad \text{onde} \quad NA = n \sin \theta$$

NA é a abertura numérica, e n o índice de refração entre a amostra e a lente. Se as duas NAs forem iguais $R = 0.61\lambda/NA$

Microscópio Óptico
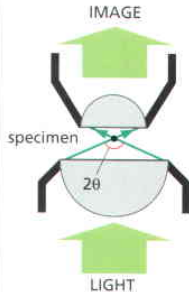
LENSES

the objective lens collects a cone of light rays to create an image

the condenser lens focuses a cone of light rays onto each point of the specimen

RESOLUTION: the resolving power of the microscope depends on the width of the cone of illumination and therefore on both the condenser and the objective lens. It is calculated using the formula

$$resolution = \frac{0.61 \, \lambda}{n \, \sin \theta}$$

where:

θ = half the angular width of the cone of rays collected by the objective lens from a typical point in the specimen (since the maximum width is 180°, $\sin \theta$ has a maximum value of 1)

n = the refractive index of the medium (usually air or oil) separating the specimen from the objective and condenser lenses

λ = the wavelength of light used (for white light a figure of 0.53 μm is commonly assumed)

NUMERICAL APERTURE: $n \sin \theta$ in the equation above is called the numerical aperture of the lens (NA) and is a function of its light-collecting ability. For dry lenses this cannot be more than 1, but for oil-immersion lenses it can be as high as 1.4. The higher the numerical aperture, the greater the resolution and the brighter the image (brightness is important in fluorescence microscopy). However, this advantage is obtained at the expense of very short working distances and a very small depth of field.
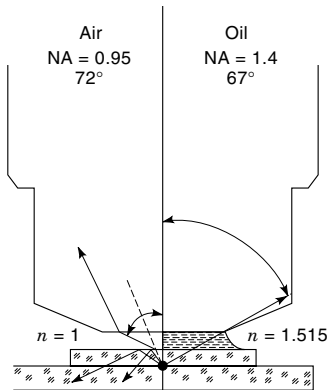
Figure 6-2

Effect of immersion oil on increasing the angular extent over which diffracted rays can be accepted by an objective lens. Numerical aperture is directly dependent on the wavelength λ and the sine of the half angle of the cone of illumination θ accepted by the front lens of the objective. For dry lenses, NA is limited, because rays subtending angles of 41° or greater are lost by total internal reflection and never enter the lens (dotted line). The practical limit for a dry lens is ~39°, which corresponds to an acceptance angle of 72°, and an NA of 0.95. By adding high-refractive index immersion oil matching that of the glass coverslip ($n = 1.515$), an oil immersion objective can collect light diffracted up to 67°, which corresponds to NA = 1.4.
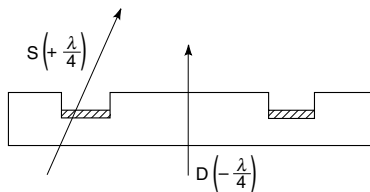
Figure 7-7

The action of a phase plate at the rear surface of the objective lens. Surround or background rays (S) are advanced in phase relative to the D wave by $\lambda/4$ at the phase plate. Relative phase advancement is created by etching a ring in the plate that reduces the physical path taken by the S waves through the high-refractive-index plate. Since diffracted object rays (D) are retarded by $\lambda/4$ at the specimen, the optical path difference between D and S waves upon emergence from the phase plate is $\lambda/2$, allowing destructive interference in the image plane. The recessed ring in the phase plate is made semitransparent so that the amplitude of the S wave is reduced by 70–75% to optimize contrast in the image plane.
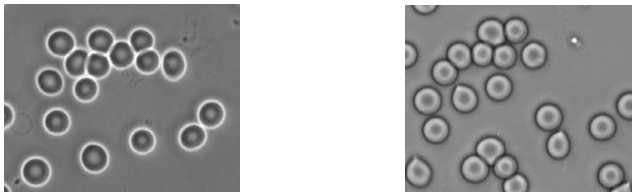
Figure 7-8

Comparison of positive and negative phase contrast systems. Shown in pairs, from the top down: phase plates for advancing (positive contrast) or retarding (negative contrast) the surround wave; amplitude profiles of waves showing destructive interference (positive phase contrast) and constructive interference (negative phase contrast) for a high-refractive-index object. Notice that the phase plate advances or retards the S wave relative to the D wave. The amplitude of the resultant P wave is lower or higher than the S wave, causing the object to look relatively darker or brighter than the background. Vector diagrams showing advancement of the S wave by $\lambda/4$, which is shown as a 90° counterclockwise rotation in positive phase contrast, and retardation of the S wave by $\lambda/4$, which is shown as a 90° clockwise rotation in negative phase contrast. Addition of the S and D wave vectors gives P waves whose amplitudes vary relative to the S waves. Images of erythrocytes in positive and negative phase contrast optics.
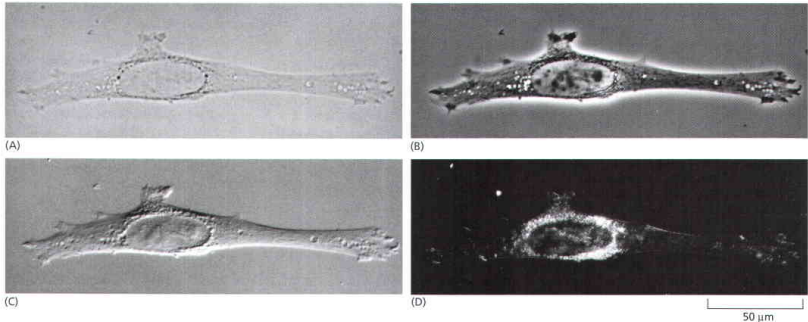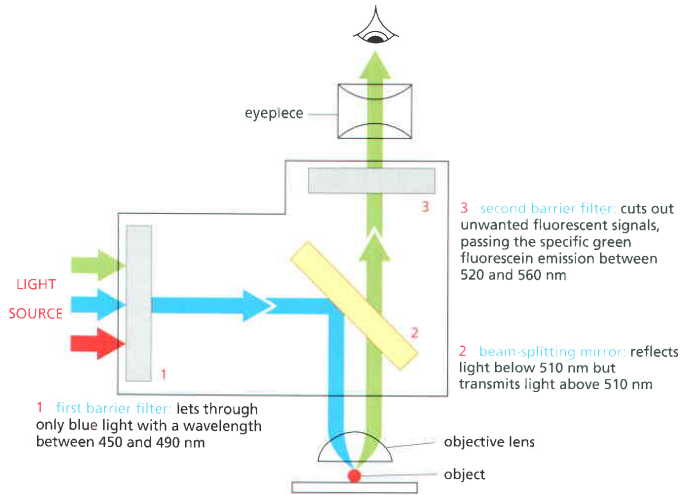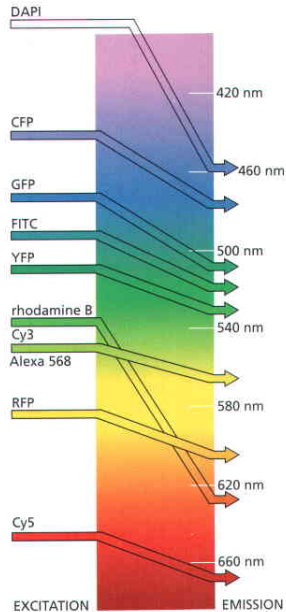
Figure 9–8 **Four types of light microscopy.** Four images are shown of the same fibroblast cell in culture. All images can be obtained with most modern microscopes by interchanging optical components. (A) Bright-field microscopy. (B) Phase-contrast microscopy. (C) Nomarski differential-interference-contrast microscopy. (D) Dark-field microscopy.

Microscópio de Fluorecência

eyepiece

3 second barrier filter: cuts out unwanted fluorescent signals, passing the specific green fluorescein emission between 520 and 560 nm

LIGHT
SOURCE

2 beam-splitting mirror: reflects light below 510 nm but transmits light above 510 nm

1 first barrier filter: lets through only blue light with a wavelength between 450 and 490 nm
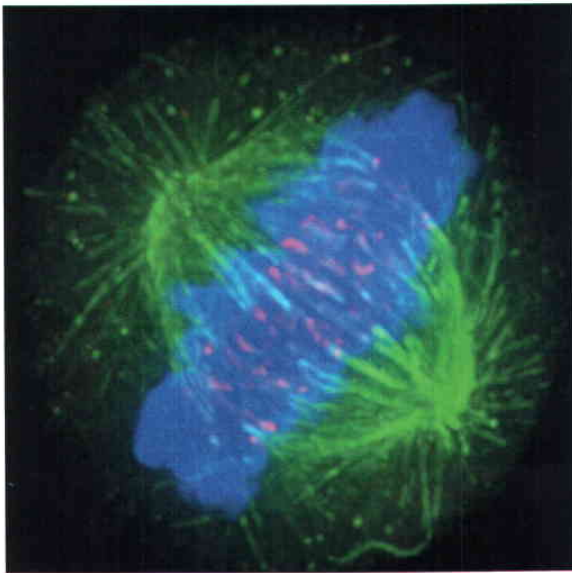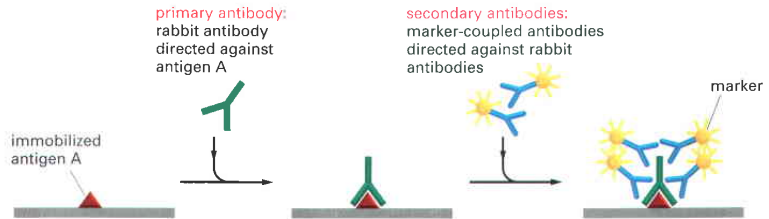
objective lens

object

Figure 9–15 Multiple-fluoresc
microscopy. In this composite
micrograph of a cell in mitosis,
different fluorescent probes ha
used to stain three different ce
components. <GTCT> The spir
microtubules are revealed with
fluorescent antibody, centrom
red fluorescent antibody and t
the condensed chromosomes
blue fluorescent dye DAPI (Co

primary antibody:
rabbit antibody
directed against
antigen A

secondary antibodies:
marker-coupled antibodies
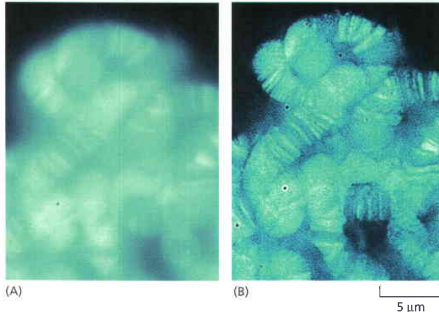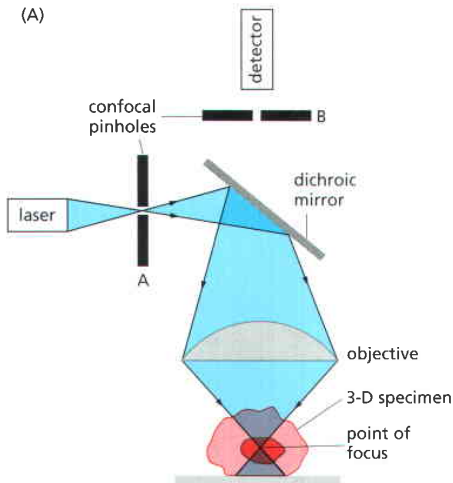directed against rabbit
antibodies

marker

immobilized
antigen A

Figure 9–19 Image deconvolution.
(A) A light micrograph of the large polytene chromosomes from Drosophi stained with a fluorescent DNA-bindin dye. (B) The same field of view after image deconvolution clearly reveals th banding pattern on the chromosomes Each band is about 0.25 μm thick, approaching the resolution limit of th light microscope. (Courtesy of the Joh Sedat Laboratory.)

(A)

(B)

5 μm

(A)

detector

confocal
pinholes · · · · · · · · · · B

dichroic
mirror

laser

A

objective

3-D specimen

point of
focus

fluorescent specimen is illuminated
with a focused point of light from
a pinhole

(B)

detector

(C)

detector

emitted fluorescent
light from in-focus
point is focused at
pinhole and reaches

emitted light from out-
of-focus point is out of
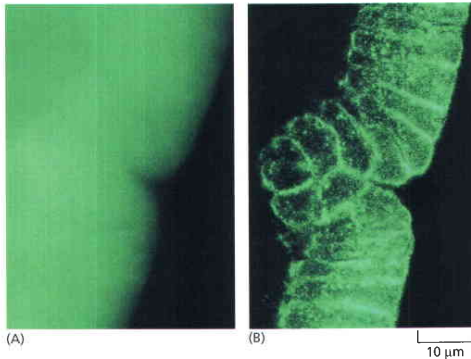focus at pinhole and
is largely excluded

(A)

(B)

|_____|
10 µm

Figure 9–21 Conventional and confocal fluorescence microscopy compared. These two micrographs are of the same intact gastrula-stage *Drosophila* embryo that has been stained with a fluorescent probe for actin filaments. (A) The conventional, unprocessed image is blurred by the presence of fluorescent structures above and below the plane of focus. (B) In the confocal image, this out-of-focus information is removed, resulting in a crisp optical section of the cells in the embryo. (Courtesy of Richard Warn and Peter Shaw.)
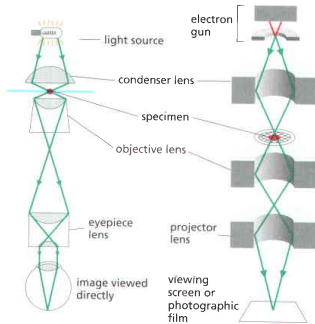
20 µm
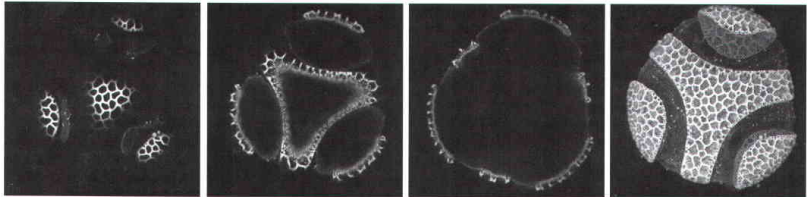
Figure 9–42 **The principal features of a light microscope and a transmission electron microscope.** These drawings emphasize the similarities of overall design. Whereas the lenses in the light microscope are made of glass, those in the electron microscope are magnetic coils. The electron microscope requires that the specimen be placed in a vacuum. The inset shows a transmission electron microscope in use. (Photograph courtesy of FEI Company Ltd.)
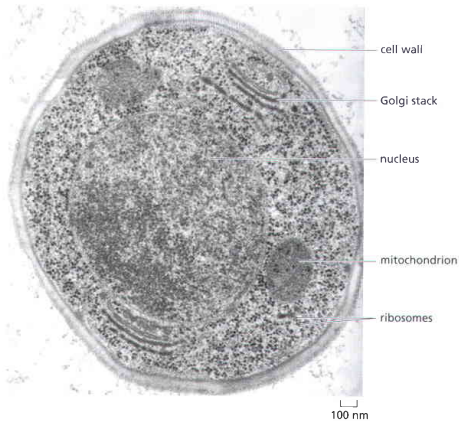
cell wall

Golgi stack

nucleus

mitochondrion

ribosomes

100 nm

Figure 9–45 Thin section of a cell. This thin section is of a yeast cell that has been very rapidly frozen and the vitreous ice replaced by organic solvents and then by plastic resin. The nucleus, mitochondria, cell wall, Golgi stacks, and ribosomes can all be readily seen in a state that is presumed to be as life-like as possible. (Courtesy of Andrew Staehelin.)
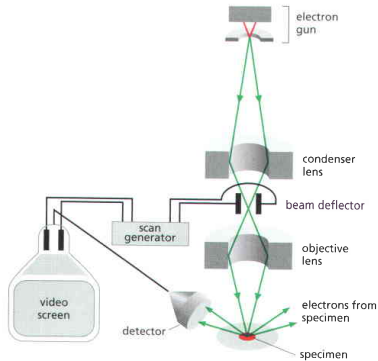
Figure 9–49 The scanning electron microscope. In a SEM, the specimen is scanned by a beam of electrons brought to a focus on the specimen by the electromagnetic coils that act as lenses. The detector measures the quantity of electrons scattered or emitted as the beam bombards each successive point on the surface of the specimen and controls the intensity of successive points in an image built up on a video screen. The SEM creates striking images of three-dimensional objects with great depth of focus and a resolution between 3 nm and 20 nm depending on the instrument. (Photograph courtesy of Andrew Davies.)
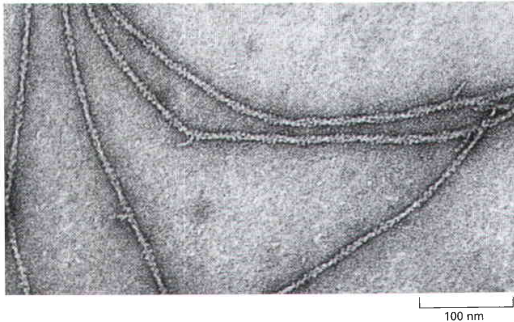
Figure 9–54 **Negatively stained actin filaments.** In this transmission electron micrograph, each filament is about 8 nm in diameter and is seen, on close inspection, to be composed of a helical chain of globular actin molecules. (Courtesy of Roger Craig.)

100 nm